

# Nanocellulose-based Translucent Diffuser for Optoelectronic Device Applications with Dramatic Improvement of Light Coupling

Wei Wu,<sup>\*,†</sup> Nancy G. Tassi,<sup>†</sup> Hongli Zhu,<sup>‡</sup> Zhiqiang Fang,<sup>‡</sup> and Liangbing Hu<sup>\*,‡</sup>

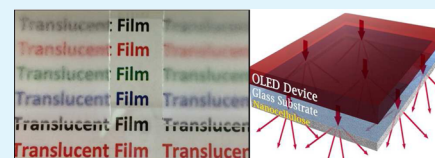
<sup>†</sup>DuPont Central Research and Development, Wilmington, Delaware 19880, United States

<sup>‡</sup>Department of Materials Science and Engineering, University of Maryland, College Park, Maryland 20740, United States

## Supporting Information

**ABSTRACT:** Nanocellulose is a biogenerated and biorenewable organic material. Using a process based on 2,2,6,6-tetramethylpiperidine-1-oxyl (TEMPO)/NaClO/NaBr system, a highly translucent and light-diffusive film consisting of many layers of nanocellulose fibers and wood pulp microfibrils was made. The film demonstrates a combination of large optical transmittance of ~90% and tunable diffuse transmission of up to ~78% across the visible and near-infrared spectra. The detailed characterizations of the film indicate the combination of high optical transmittance and haze is due to the film's large packing density and microstructured surface. The superior optical properties make the film a translucent light diffuser and applicable for improving the efficiencies of optoelectronic devices such as thin-film silicon solar cells and organic light-emitting diodes.

**KEYWORDS:** nanocellulose, diffuser, thin film, optoelectronics, organic lighting emitting diodes, solar cells



## INTRODUCTION

Nanocellulose as a biogenerated and biorenewable material has recently attracted a lot of interests and development efforts due to its exciting properties and potential applications.<sup>1–5</sup> It can be extracted from many cellulose-containing materials with the most common source being woods. Natural wood fibers have unique hierarchical and hollow structure.<sup>6,7</sup> One tracheid cell wall is composed of dozens of nanofibers.<sup>8,9</sup> Using mechanical methods such as homogenizer, microfluidizers, and grinders, nanocellulose fibers can be fibrillated from the wood-based pulps.<sup>10–12</sup> However, the mechanical processes consume large amounts of energy. To reduce the energy consumption, different methods such as enzymatic pretreatment,<sup>13,14</sup> carboxymethylation,<sup>15</sup> and 2,2,6,6-tetramethylpiperidine-1-oxyl (TEMPO)-mediated oxidation<sup>16–19</sup> have been introduced. TEMPO can selectively oxidize the hydroxyl group at C6 in the glucose unit to carboxyl group. The tracheid cell wall in the wood pulps is swelled, corrupted, and even partially unzipped after the TEMPO treatment. The TEMPO-processed nanocellulose film (NCF) has very fine fiber diameters (5–20 nm) and a large packing density. The cavities initially existing between the neighboring native wood pulps can be dramatically removed. Therefore, the NCF film can achieve a very high optical transparency.<sup>20</sup> Nanocellulose film made of different diameters of nanocellulose fibers can also show a large haze due to the light scattering of the nanofibers.<sup>21</sup>

Here, we present our original optical characterizations of a thin film made of TEMPO-treated nanocellulose fibers mixed with wood pulp microfibrils as a translucent diffuser and their potential application to couple the light in solar cells and organic light emitting diodes (OLED). The hybrid film shows a large optical transmittance of ~90% across the visible and near-infrared spectra, and a tunable diffuse transmission of up to

~78%. The superior optical properties are attributed to the film's large packing density and microstructured surface. The accelerated UV exposure applied on the film also indicates the UV stability of the film. Films or substrates with such high optical transmittance and haze are useful for improving the optoelectronic devices. For example, thin-film crystalline Si solar cells have the advantages of using less materials and requiring lower quality (carrier diffuse length relaxation) in comparison to the standard thick Si solar cells. However, one major issue for thin-film Si is the incomplete light absorption.<sup>22</sup> The conventional pyramidal textures on the Si surface require the roughness of a few micrometers and alkaline solution etching, both of which are difficult for the very thin Si films.<sup>23,24</sup> Plasmonic nanostructures can be applied to enhancing the light absorption of the Si thin-film solar cells.<sup>25–27</sup> However, these structures generate light absorption which converts to heat waste, and the fabrication processes for the nanostructures are not cost-effective. Here, we use the nanocellulose-based film as a translucent diffuser to increase the thin-film Si's light absorption and photon-current density. Another example is to enhance the light outcoupling efficiency of OLED lighting device. Due to the refractive index mismatch between the standard glass substrate and air, about 20% power of the output light is trapped in the glass substrate as the substrate modes.<sup>28</sup> Different techniques such as applying microlens array, adding a light-scattering layer and applying low-index silica aerogel have been applied to improving the light extraction.<sup>29–31</sup> Here, we apply the light-diffusive film made of nanocellulose as the light

Received: September 30, 2015

Accepted: November 17, 2015

Published: November 17, 2015

extraction layer on the glass substrate and improve the illuminous efficacy by almost 15%.

## EXPERIMENTAL SECTION

Wood pulps were from a bleached sulfate soft wood pulp (Southern Yellow Pine). They were dispersed in distilled water with a concentration of 1% in which sodium bromide and TEMPO were dissolved (10.0 and 1.6 wt % respectively). The nanocellulose fibers were fibrillated based on TEMPO-mediated oxidization and homogenization. Detailed nanofibrillation processes can be found in previous references.<sup>32,33</sup> A high-pressure homogenization procedure with a Microfluidizer processor M110EH (from Microfluidics Ind.) was applied in the process. The mixed suspension was formed by dispersing the wood pulps into 0.1 wt % nanocellulose fibers suspension, and stirred for 10 min to form uniform hybrid dispersion. The suspension was then drop-coated on a clean glass substrate and was dried for overnight at room temperature. To form an even thicker coating, we dropped another suspension onto the surface of the coating again. To form a thicker translucent film without any substrate, we filtered and dried the suspension between two filter papers under pressure at room temperature.

The optical transmission and reflection spectra were measured with an integrated sphere setup using the spectrometer Lambda 900 UV/vis/NIR spectrometer. 3-D optical surface profilometry was performed on the film using Zygo NewView 5000 model. The height range is from 1 nm to 5 mm, and the lateral range is from slightly less than 1  $\mu\text{m}$  to centimeter (cm) scale if necessary. Mercury intrusion porosimetry was conducted on the samples to assess porosity in the 3 nm–400  $\mu\text{m}$  region. Outgassed samples were charged to the calibrated penetrometer cell of the Micromeritics AutoPore III. The penetrometer was sealed, installed in the instrument and placed under vacuum. Mercury was admitted to the penetrometer at gradually increasing pressure from 0 to 413 MPa (0–60 000 psia) and intrusion was recorded (64 data points) and analyzed via the Washburn Equation with a contact angle value of 130° and surface tension of 485 dyn/cm to generate pore size/volume distribution.<sup>34</sup> The porosity is calculated by

$$\text{porosity (\%)} = \frac{\sum_a^b V}{\Delta V_T + \frac{1}{\rho}} \times 100$$

where  $\sum V$  is the sum of the volume increments over the pore size range of interest,  $\Delta V_T$  is the total pore volume, and  $\rho$  is the density of the sample.

For light scattering applications for solar cell devices, we purchased a superthin flexible Si wafer ( $\sim 10 \mu\text{m}$  thick) from Virginia Semiconductor, Inc. The wafer was optically smooth on both sides, and only partially absorbed the sun light due to the limited thickness. The diameter of the wafer is 1 in. The translucent film was coated on the thin wafer supported by a glass slide with the aid of a drop of the mixed suspension. The light absorption spectra of the wafer were measured before and after applying the mixed nanocellulose solution on the surface of the wafer. The photocurrent densities generated by the Si wafers were calculated using semiconducting thin film optics simulation software (Fluxim, Inc.). To apply the film for OLED outcoupling improvement, the film was laminated on the glass substrate using index-match oil ( $n \sim 1.5$ ). The OLED device was fabricated within DuPont. Before and after applying the film, the characteristics of the OLED device including current density-bias voltage and luminous efficacy-bias voltage were measured. The wavelength of the OLED light was 560 nm (green light), and the pixel area was 94  $\text{mm}^2$ .

## RESULTS AND DISCUSSION

The mixed nanocellulose and wood pulp solutions and films are made from the southern yellow pine soft wood pulps based on the TEMPO/NaClO/NaBr process. (The detailed experimental steps are found in the [Experimental Section](#).) Films of

different thicknesses are formed by coating and drying nanocellulose solutions on a piece of standard glass slide substrate. The translucent film without substrate is formed by drying between two filter papers under pressure at room temperature. Visible and near-infrared spectroscopic measurements are applied to measuring the transmission and reflection spectra of the samples. [Figure 1a](#) shows the total and diffuse

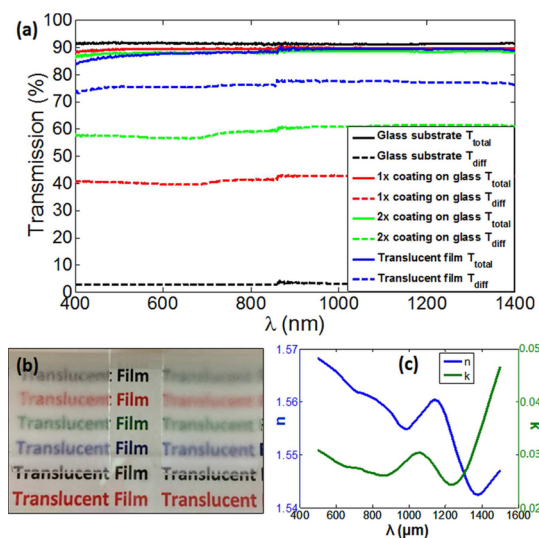


**Figure 1.** (a) Total transmission and diffuse transmission spectra for different coatings of nanocellulose-based film on glass substrate and nanocellulose-based translucent film; (b) two different thicknesses of film coatings on glass substrates illustrating the translucent effect; (c) the optical constants of the translucent film by ellipsometry spectroscopic measurement.

transmission spectra of two different thicknesses of nanocellulose films (average thicknesses of  $\sim 10$  and  $\sim 20 \mu\text{m}$ ) on glass substrates, and a thick translucent film (average thickness of  $\sim 40 \mu\text{m}$ ) without a substrate. All the translucent coatings and film have shown a very high total transmission (solid red, green, and blue lines) which is close to that of a glass substrate (solid black line) due to the close match of refractive index with glass substrate. On the basis of our angled spectroscopic ellipsometry measurement ([Figure 1c](#)), the refractive index of the coated nanocellulose film is  $\sim 1.56$  in the visible region, which is close to the glass ( $n \sim 1.45$ ). The red, green, and blue dash lines show the measured diffuse transmission for the three samples. By varying the thicknesses of the films (the numbers of coating layers), the diffuse transmission (or haze) can be significantly tuned. The diffuse transmission can reach as large as  $\sim 78\%$  by forming a thick translucent film. The haze of the films is mostly originated from the light scatterings due to the surface roughness of films, which will be further discussed below. [Figure S1 \(Supporting Information\)](#) shows typical three-dimensional (3-D) height mapping and the extracted root-mean square (rms) of surface roughness of the three films' surfaces using optical profilometer. The rms of the films is in the range of 2–5  $\mu\text{m}$ , and the diffuse transmission increases as the surface roughness increase. The lowest black dashed line shows the diffuse transmission of the glass substrate, which is close to zero (mostly including the diffuse transmission from both glass substrate and instrument error). The optical absorption of all these samples is also measured and very close to zero, which is expected because cellulose has no light

absorption in the visible and near-IR regions.<sup>35</sup> Figure 1b shows an example of the two different translucent coatings on glass substrates illustrating the transparent and haze effect.

To understand the large optical transmission and diffuse transmission, both top and cross-sectional scanning electron microscope (SEM) images have been taken on the coated film on the glass substrate (Figure 2a–c). On the surface of the film,

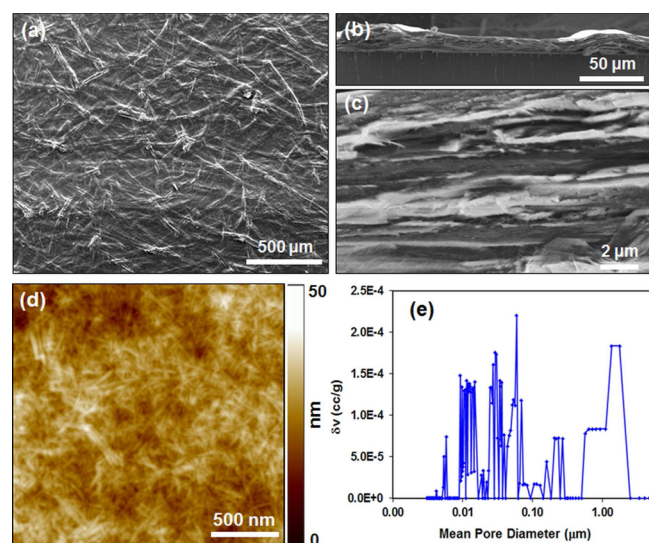


**Figure 2.** (a) SEM top view of the hybrid film made of nanocellulose fibers and wood pulps; (b) SEM cross-sectional view of the hybrid film on a glass substrate; (c) enlarged SEM cross-sectional view of image b; (d) AFM height view of the nanocellulose fibers between the wood pulps; (e) mean pore diameter distributions of the translucent film measured by mercury intrusion porosimetry.

the microscale wood pulps (diameters of  $\sim 20$ – $40 \mu\text{m}$ ) can be clearly seen. The random distributions of them result in the film's surface roughness which is good for light forward-scattering and diffusion. Nanocellulose fibers (diameters of  $\sim 5$ – $20 \text{ nm}$ ) are filling the microcavities between the wood pulps, which helps avoid the backward light scattering and reflection. From the SEM cross-sectional views, the film seems to have dense layered structures. It also shows a microscale thickness fluctuation due to the random distributions of wood pulps. Figure 2c shows the enlarged SEM view of the film. Very dense layered structures containing the nanoscale fibers can be seen. Figure 2d is the atomic force microscope (AFM) height view of the surface area between the wood pulps. The nanocellulose fibers have very small diameters (comparing to the wavelengths of the visible light) and are very densely packed which reduces the pores in the film. On the basis of AFM height data, the surface roughness of the nanocellulose fibers is only  $\sim 4.4 \text{ nm}$ . Mercury intrusion porosimetry has also been applied to measuring the porosity of the translucent film. Figure 2e shows the extracted mean pore diameter distributions of the translucent film. As expected, the film shows very small volumes of the microscale and nanoscale pores. The measured skeletal density (after compressibility correction) of the film is  $\sim 1.58 \text{ g cm}^{-3}$ , and the calculated internal porosity of the film including all the pores with the diameters from  $3 \text{ nm}$  to  $5 \mu\text{m}$  is only  $\sim 0.6\%$ . This result confirms that the film has a very large packing density due to the filling of the nanocellulose fibers, and the dense film results in a very large optical transmission and avoids the strong back-forward light scattering found

within a normal paper. It is generally known that there are two routes to obtain or increase organic film haze: (1) by inhomogeneous internal scattering and (2) by surface scattering, such as surface roughness.<sup>36</sup> The highly dense nature of the film indicates that the strong light scattering is due to the surface scattering caused by the surface roughness from the microscale wood pulp fibers.

Because of the large total and diffuse light transmission, the translucent film can be applied to increasing the light's path length in the thin-film crystalline Si film and improving the light absorption especially for the long wavelength which has smaller absorption coefficients. Figure 3a shows a schematic of the nanocellulose translucent film coated on the thin Si wafer to illustrate the light trapping effect. Figure 3b shows the measured light absorption spectra by a  $10 \mu\text{m}$  thick ultrathin and smooth Si wafer with and without the nanocellulose film coating  $\sim 40 \mu\text{m}$  thick. With the translucent diffuser on the surface of the ultrathin Si wafers, the light absorption is clearly improved. Assuming the carrier collection efficiency to be one for such a thin silicon wafer, the photocurrent current density can be calculated by integrating the light absorption spectra with Solar AM 1.5G spectrum. Figure 3c shows the calculated photocurrent densities generated from different thicknesses of Si with and without the translucent film. Due to the increased light path length inside the thin Si wafer and the reduced reflection, the photocurrent density can be improved by  $\sim 13\%$ . The UV stability is critical for translucent films being applied in solar cells. The film has been tested under  $50\times$  concentrated solar lamp to accelerate the UV exposure. The total transmission and diffuse transmission spectra of the film under different hours of exposure are shown in Figure 3d. The results have shown that the film is stable even after 12 h of continuous exposure at an intensity of 50 Suns, which indicates the film's UV stability. The translucent film composed of wood pulps and nanocellulose fibers also has a good thermal stability up to  $200 \text{ }^\circ\text{C}$ .<sup>37</sup> The excellent UV, thermal stability and strong translucency of the film are beneficial for solar cell applications.

The translucent diffuser can also be applied to improving the light extraction from OLED device because of its strong light transmittance and scattering properties. The translucent film of  $\sim 40 \mu\text{m}$  thickness has also been applied on the rear side of the glass substrate of a finished OLED device emitting green light ( $\sim 560 \text{ nm}$ ) with the aid of index matching oil ( $n \sim 1.5$ ). Before and after the film's coating, there is no difference for the intrinsic performance of the OLED device. Figure 4a shows the current density–voltage curves of the device with and without the film (inset shows the schematics of the translucent film as an outcoupling layer on the OLED). Due to the improved light extraction, the device's light output power and luminous efficacy are improved (Figure 4b). The largest efficacy improvement is almost 15% (from  $\sim 56.77 \text{ lm/W}$  to  $\sim 65.12 \text{ lm/W}$ ) at the bias of  $\sim 2.4 \text{ V}$  with the film coated on the substrate. This method is useful for improving the OLED efficacy for the application of lighting. Comparing with other light outcoupling methods, the fabrication process is large scalable, low cost, and the material used is earth abundant and sustainable. The improvement mechanism for OLED devices is mostly due to the translucent film's strong light diffusion property, which helps extract the trapped light more efficiently. This method of combining nanocellulose-based film with glass substrate also has the advantages of maintaining the glass substrate's smoothness and barrier properties to benefit OLED

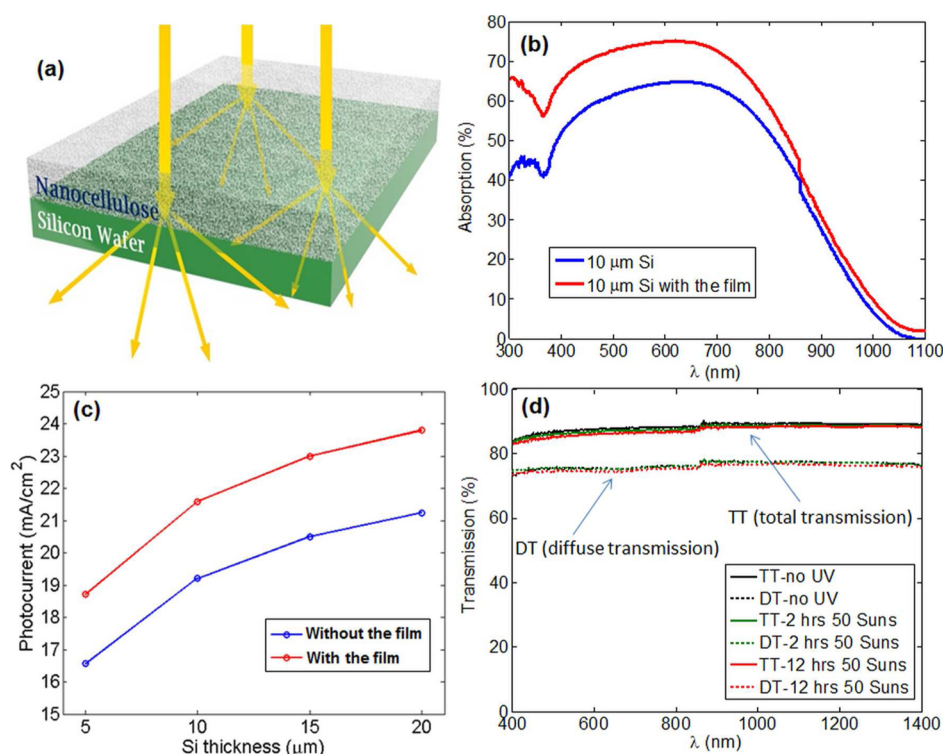


**Figure 3.** (a) Schematic illustration of the nanocellulose translucent film coated on the thin Si wafer to illustrate the light trapping effect; (b) absorption spectra of 10  $\mu\text{m}$  thick, smooth Si wafer with and without the nanocellulose-based film coating; (c) calculated photocurrent densities with different thicknesses with and without the film; and (d) total and diffuse transmission spectra of nanocellulose-based film under an intensity of 50 Suns for different lengths of time.

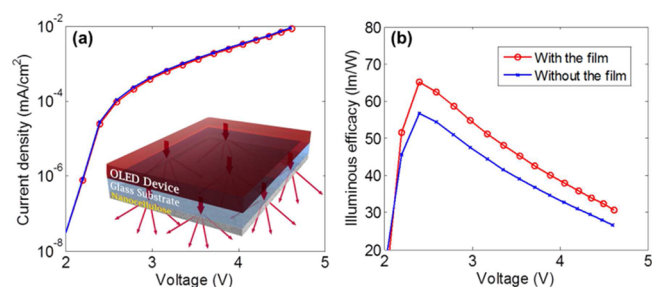


**Figure 4.** (a) Current density–voltage curves of a green OLED device with and without nanocellulose-based film being applied on the rear side of the glass substrate; (b) illuminous efficacy–voltage curves with and without the film.

devices, in comparison to previously reported method of using only nanocellulose film as a substrate.<sup>38–40</sup>

## CONCLUSIONS

We have presented a nanocellulose-based film as a strong optical translucent diffuser. The film is made of nanocellulose fibers and wood pulp microfibrils. Due to the large packing density and microstructured surface, the film exhibits a large optical transmittance of  $\sim 90\%$  with a tunable diffuse transmission up to 78%. The superior combination makes it useful for applications of many optoelectronic devices, such as improving the light absorption of thin-film silicon solar cells and light extraction of OLED devices.

## ASSOCIATED CONTENT

### Supporting Information

The Supporting Information is available free of charge on the ACS Publications website at DOI: 10.1021/acsami.5b09249.

3D optical profilometry height view and comparisons of extracted root-mean square (rms) of surface roughness. (PDF)

## AUTHOR INFORMATION

### Corresponding Authors

\*E-mail: [wei.wu@dupont.com](mailto:wei.wu@dupont.com).

\*E-mail: [binghu@umd.edu](mailto:binghu@umd.edu).

### Notes

The authors declare no competing financial interest.

## ACKNOWLEDGMENTS

The authors at DuPont would like to thank our colleagues Alan Allgeier, Jing Li, Keith Warrington, and Lei Zhang at the DuPont Corporate Center for Analytical Science for the assistance of film characterizations. We also thank our colleagues Michael Lemon for the assistance of ellipsometry measurement and Ian Parker for OLED device characterization. We are also grateful for the consistent support and guidance from Salah Boussaad, D. Neil Washburn, and Steve Freilich. The authors at UMD acknowledge the support from DOD (Air Force of Scientific Research) Young Investigator Program (FA95501310143).

## REFERENCES

- Eichhorn, S. J.; Dufresne, A.; Aranguren, M.; Marcovich, N. E.; Capadona, J. R.; Rowan, S. J.; Weder, C.; Thielemans, W.; Roman, M. J.

- Rennecker, S.; Gindl, W.; Veigel, S.; Keckes, J.; Yano, H.; Abe, K.; Nogi, M.; Nakagaito, A. N.; Mangalam, A.; Simonsen, J.; Benight, A. S.; Bismarck, A.; Berglund, L. A.; Peijs, T. Review: Current International Research into Cellulose Nanofibres and Nanocomposites. *J. Mater. Sci.* **2010**, *45*, 1–33.
- (2) Moon, R. J.; Martini, A.; Nairn, J.; Simonsen, J.; Youngblood, J. Cellulose Nanomaterials Review: Structure, Properties and Nanocomposites. *Chem. Soc. Rev.* **2011**, *40*, 3941–3994.
- (3) Chirayil, C. J.; Mathew, L.; Thomas, S. Review of Recent Research in Nano Cellulose Preparation from Different Lignocellulosic Fibers. *Rev. Adv. Mater. Sci.* **2014**, *37*, 20–28.
- (4) Siró, I.; Plackett, D. Microfibrillated Cellulose and New Nanocomposite Materials: a Review. *Cellulose* **2010**, *17*, 459–494.
- (5) Klemm, D.; Kramer, F.; Moritz, S.; Lindström, T.; Ankerfors, M.; Gray, D.; Dorris, A. Nanocelluloses: A New Family of Nature-Based Materials. *Angew. Chem., Int. Ed.* **2011**, *50*, 5438–5466.
- (6) Postek, M. T.; Vladár, A.; Dagata, J.; Farkas, N.; Ming, B.; Wagner, R.; Raman, A.; Moon, R. J.; Sabo, R.; Wegner, T. H.; Beecher, J. Development of the Metrology and Imaging of Cellulose Nanocrystals. *Meas. Sci. Technol.* **2011**, *22*, 024005–024015.
- (7) Isogai, A.; Saito, T.; Fukuzumi, H. TEMPO-Oxidized Cellulose Nanofibers. *Nanoscale* **2011**, *3*, 71–85.
- (8) Heyn, A. N. J. The Elementary Fibril and Supermolecular Structure of Cellulose in Soft Wood Fiber. *J. Ultrastruct. Res.* **1969**, *26*, 52–68.
- (9) González, I.; Alcalá, M.; Chinga-Carrasco, G.; Vilaseca, F.; Boufi, S.; Mutjé, P. From Paper to Nanopaper: Evolution of Mechanical and Physical Properties. *Cellulose* **2014**, *21*, 2599–2609.
- (10) Andresen, M.; Johansson, L.-S.; Tanem, B. S.; Stenius, P. Properties and Characterization of Hydrophobized Microfibrillated Cellulose. *Cellulose* **2006**, *13*, 665–677.
- (11) Abdul Khalil, H. P. S.; Bhat, A. H.; Ireana Yusra, A. F. Green Composites from Sustainable Cellulose Nanofibrils: A Review. *Carbohydr. Polym.* **2012**, *87*, 963–979.
- (12) Lavoine, N.; Desloges, I.; Dufresne, A.; Bras, J. Microfibrillated Cellulose – Its Barrier Properties and Applications in Cellulosic Materials: A Review. *Carbohydr. Polym.* **2012**, *90*, 735–764.
- (13) Pääkkö, M.; Ankerfors, M.; Kosonen, H.; Nykänen, A.; Ahola, S.; Österberg, M.; Ruokolainen, J.; Laine, J.; Larsson, P. T.; Ikkala, O.; Lindström, T. Enzymatic Hydrolysis Combined with Mechanical Shearing and High-Pressure Homogenization for Nanoscale Cellulose Fibrils and Strong Gels. *Biomacromolecules* **2007**, *8*, 1934–1941.
- (14) Henriksson, M.; Henriksson, G.; Berglund, L. A.; Lindström, T. An Environmentally Friendly Method for Enzyme-Assisted Preparation of Microfibrillated Cellulose (MFC) Nanofibers. *Eur. Polym. J.* **2007**, *43*, 3434–3441.
- (15) Wågberg, L.; Decher, G.; Norgren, M.; Lindström, T.; Ankerfors, M.; Axnäs, K. The Build-Up of Polyelectrolyte Multilayers of Microfibrillated Cellulose and Cationic Polyelectrolytes. *Langmuir* **2008**, *24*, 784–795.
- (16) Saito, T.; Isogai, A. TEMPO-Mediated Oxidation of Native Cellulose. The Effect of Oxidation Conditions on Chemical and Crystal Structures of the Water-Insoluble Fractions. *Biomacromolecules* **2004**, *5*, 1983–1989.
- (17) Isogai, A.; Kato, Y. Preparation of Polyuronic Acid from Cellulose by TEMPO-mediated Oxidation. *Cellulose* **1998**, *5*, 153–164.
- (18) Wu, C.-N.; Yang, Q.; Takeuchi, M.; Saito, T.; Isogai, A. Highly Tough and Transparent Layered Composites of Nanocellulose and Synthetic Silicate. *Nanoscale* **2014**, *6*, 392–9.
- (19) Saito, T.; Okita, Y.; Nge, T. T.; Sugiyama, J.; Isogai, A. TEMPO-Mediated Oxidation of Native Cellulose: Microscopic Analysis of Fibrous Fractions in the Oxidized Products. *Carbohydr. Polym.* **2006**, *65*, 435–440.
- (20) Fukuzumi, H.; Saito, T.; Iwata, T.; Kumamoto, Y.; Isogai, A. Transparent and High Gas Barrier Films of Cellulose Nanofibers Prepared by TEMPO-Mediated Oxidation. *Biomacromolecules* **2008**, *10*, 162–165.
- (21) Zhu, H.; Parvinian, S.; Preston, C.; Vaaland, O.; Ruan, Z.; Hu, L. Transparent Nanopaper with Tailored Optical Properties. *Nanoscale* **2013**, *5*, 3787–3792.
- (22) Bozzola, A.; Kowalczewski, P.; Andreani, L. C. Towards High Efficiency Thin-Film Crystalline Silicon Solar Cells. *J. Appl. Phys.* **2014**, *115*, 094501.
- (23) Zeman, M.; Isabella, O.; Jäger, K.; Santbergen, R.; Solntsev, S.; Topic, M.; Krc, J. Advanced Light Management Approaches for Thin-Film Silicon Solar Cells. *Energy Procedia* **2012**, *15*, 189–199.
- (24) Brongersma, M. L.; Cui, Y.; Fan, S. Light Management for Photovoltaics Using High-Index Nanostructures. *Nat. Mater.* **2014**, *13*, 451–460.
- (25) Spinelli, P.; Ferry, V. E.; Van De Groep, J.; Van Lare, M.; Verschuuren, M. A.; Schropp, R. E. L.; Atwater, H. A.; Polman, A. Plasmonic Light Trapping in Thin-Film Si Solar Cells. *J. Opt.* **2012**, *14*, 024002.
- (26) Atwater, H. A.; Polman, A. Plasmonics for Improved Photovoltaic Devices. *Nat. Mater.* **2010**, *9*, 205–213.
- (27) Wang, P. H.; Millard, M.; Brolo, A. G. Optimizing Plasmonic Silicon Photovoltaics with Ag and Au Nanoparticle Mixtures. *J. Phys. Chem. C* **2014**, *118*, 5889–5895.
- (28) Meerheim, R.; Furno, M.; Hofmann, S.; Lüssem, B.; Leo, K. Quantification of Energy Loss Mechanisms in Organic Light Emitting Diodes. *Appl. Phys. Lett.* **2010**, *97*, 253305.
- (29) Möller, S.; Forrest, S. R. Improved Light Out-Coupling in Organic Light Emitting Diodes. *J. Appl. Phys.* **2002**, *91*, 3324–3327.
- (30) Tsutsui, T.; Yahiro, M.; Yokogawa, H.; Kawano, K.; Yokoyama, M. Doubling Coupling-Out Efficiency in Organic Light-Emitting Diodes. *Adv. Mater.* **2001**, *13*, 1149–1152.
- (31) Nakamura, T.; Tsutsumi, N.; Juni, N.; Fujii, H. Improvement of Coupling-Out Efficiency in Organic Electroluminescent Devices by Addition of a Diffusive Layer. *J. Appl. Phys.* **2004**, *96*, 6016–6022.
- (32) Fang, Z.; Zhu, H.; Preston, C.; Han, X.; Li, Y.; Lee, S.; Chai, X.; Chen, G.; Hu, L. Highly Transparent and Writable Wood All-Cellulose Hybrid Nanostructured Paper. *J. Mater. Chem. C* **2013**, *1*, 6191–6197.
- (33) Huang, J.; Zhu, H.; Chen, Y.; Preston, C.; Rohrbach, K.; Cumings, J.; Hu, L. Highly Transparent and Flexible Nanopaper Transistors. *ACS Nano* **2013**, *7*, 2106–2113.
- (34) Webb, P. A. *An Introduction To The Physical Characterization of Materials by Mercury Intrusion Porosimetry with Emphasis on Reduction and Presentation of Experimental Data*, 1st ed; Micromeritics Instrument Corp.: Norcross, GA, 2001.
- (35) Wertz, J.-L.; Bédué, O.; Mercier, J. P. *Cellulose Science and Technology*, 1st ed; EPFL Press: Lausanne, Switzerland, 2010.
- (36) Chen, X.-Y.; Xiang, M. Formulating of a Novel Polyolefin Hazy Film and the Origins of Haze Thereof. *Polym. Bull.* **2010**, *64*, 925–937.
- (37) Dufresne, A. *Nanocellulose: From Nature to High Performance Tailored Materials*, 1st ed; Walter de Gruyter: Berlin, Germany, 2012.
- (38) Zhu, H. L.; Xiao, Z. G.; Liu, D. T.; Li, Y. Y.; Weadock, N. J.; Fang, Z. Q.; Huang, J. S.; Hu, L. B. Biodegradable Transparent Substrates for Flexible Organic-Light-Emitting Diodes. *Energy Environ. Sci.* **2013**, *6*, 2105–2111.
- (39) Okahisa, Y.; Yoshida, A.; Miyaguchi, S.; Yano, H. Optically Transparent Wood–Cellulose Nanocomposite as a Base Substrate for Flexible Organic Light-Emitting Diode Displays. *Compos. Sci. Technol.* **2009**, *69*, 1958–1961.
- (40) Purandare, S.; Gomez, E. F.; Steckl, A. J. High Brightness Phosphorescent Organic Light Emitting Diodes on Transparent and Flexible Cellulose Films. *Nanotechnology* **2014**, *25*, 094012.